Two-dimensional buoyant plumes in a uniform co-flow

Gary R. Hunt[1],† and Jamie P. Webb[1]

[1]Department of Engineering, University of Cambridge, Trumpington Street, Cambridge CB2 1PZ, UK

The behaviour of turbulent, buoyant, planar plumes is fundamentally coupled to the environment within which they develop. The effect of a background stratification directly influences a plumes buoyancy and has been the subject of numerous studies. Conversely, the effect of an ambient co-flow, which directly influences the vertical momentum of a plume, has not previously been the subject of theoretical investigation. The governing conservation equations for the case of a uniform co-flow are derived and the local dynamical behaviour of the plume is shown to be characterised by the scaled source Richardson number and the relative magnitude of the co-flow and plume source velocities. For forced, pure and lazy plume release conditions the co-flow acts to narrow the plume and reduce both the dilution and the asymptotic Richardson number relative to the classic zero co-flow case. Analytical solutions are developed for pure plumes from line sources, and for highly forced and highly lazy releases from sources of finite width in a weak co-flow. Contrary to releases in quiescent surroundings, our solutions show that all classes of release can exhibit plume contraction and the associated necking. For entraining plumes, a dynamical invariance spatially only occurs for pure and forced releases and we derive the co-flow strengths that lead to this invariance.

Key words: plumes/thermals

1. Introduction

Turbulent, buoyant, planar plumes in a steady co-flowing environment, the basic configuration for which is depicted in figure 1, have received remarkably little attention. Consequently, our understanding of these plumes is limited: the sum total of the previous investigations being those by Anwar (1969) and Rajaratnam & Lal (1983). Whilst these studies provide a first insight, the technical note of Rajaratnam & Lal (1983) presents power-law scalings for a uniform co-flow valid only in the far field of the plume and Anwar (1969) focuses on aqueous plumes in co-flows so weak that he concludes the

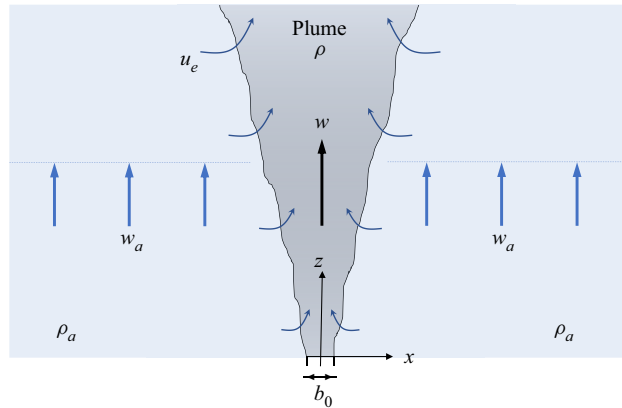† Email address for correspondence: gary.hunt@eng.cam.ac.uk

Figure 1. Schematic of a vertical section through a turbulent planar plume in a steady uniform co-flow of vertical velocity w_a and density ρ_a. The plume source, located at the coordinate origin, spans a width $-b_0/2 \leq x \leq b_0/2$.

data are well represented by the Lee & Emmons (1961) model for a plume in quiescent surroundings. Indeed, the velocity of the co-flow that Anwar (1969) considers is just one tenth of the plumes source velocity. We are unaware of any other published literature concerning the behaviour of a turbulent planar plume in a co-flow. Given this sparsity of information, later we appeal to insights that may be garnered from related, but distinct, problems − specifically, planar plumes in quiescent environments, and axisymmetric plumes and planar jets in co-flows. We approach literature on the latter with caution given it is well established that classic axisymmetric and planar plumes can exhibit markedly different behaviours, both quantitatively and qualitatively, and given that the role of buoyancy fundamentally distinguishes classic plumes from jets, providing a mechanism for increasing the momentum flux. We make no attempt to exhaustively review these fields but instead point to some of the pertinent results.

Our focus herein concerns the fundamental question of how a co-flow affects or controls planar plume behaviour. The route we take is to develop a simplified theoretical model, following the essence of the approach that underpins classic plume theory (Morton, Taylor & Turner 1956). A turbulent plume is intrinsically coupled to the environment within which it develops through the process of entrainment or detrainment. For the case of a co-flowing environment of comparable velocity to the plume source, we investigate theoretically how this coupling fundamentally alters the local dynamical behaviour from that of the corresponding plume in quiescent surroundings. To do this, we follow the procedure developed by Hunt & Kaye (2005), and applied by van den Bremer & Hunt (2014) to planar plumes in quiescent surroundings, in which the governing equations are expressed and solved in terms of the local Richardson number Γ. Specifically, we are interested in modelling how the co-flow alters the well-established behaviours of forced ($\Gamma < 1$), pure ($\Gamma = 1$) and lazy ($\Gamma > 1$) releases. Locally forced releases refer to those dominated by inertia and lazy releases to those dominated by the buoyancy force.

Turbulent buoyant plumes issuing into quiescent environments, wherein the motion of the environment is solely that induced by the plume, have been studied for over eight decades. Building on the early theoretical approach of Zeldovich (1937) and Morton *et al.* (1956) for time-averaged axisymmetric plumes from point sources, Lee & Emmons (1961) extended, what is now widely referred to as classic plume theory, to planar plumes from line sources. Numerous developments have since followed for both uniform and

stratified environments. In-depth reviews of this field are given by Turner (1966), Kaye (2008), Woods (2010) and Hunt & van den Bremer (2011). Of particular relevance to our work herein is the extension by Morton (1961) to the classic theory which considers axisymmetric turbulent plumes in a co-flow. Morton (1961) develops equations for the conservation of mass, momentum and density deficiency, and compares the resulting solutions for plumes and jets by means of 'momentum–mass flux' diagrams. While this approach is informative for the comparison of plume-like flows, it does not readily enable the influence of the co-flow on the dynamical state of the plume, i.e. whether it is locally forced, pure or lazy, to be determined. As this is one of our primary goals we adopt an alternative approach (§ 2.2), drawing from the pioneering work of Morton (1961) in developing the conservation equations relevant for a planar plume in a co-flow (§ 2).

For plumes issuing into an environment in motion, the majority of the research to date has been restricted to cross-flows, for which there are an abundance of practical examples. These include a plume from an industrial chimney issuing into a windy environment (Csanady 1965) and a buoyant discharge of pollutant into a river or an ocean current (Koh & Brooks 1975; Wood, Bell & Wilkinson 1993). The role of the cross-flow for an axisymmetric plume has been investigated theoretically by Csanady (1965), and theoretically and experimentally by Fan (1967), Hoult & Weil (1972) and Wright (1977). In contrast, there is a sparsity of literature for planar plumes in a cross-flow, however, Ramaprian & Haniu (1989) provide experimental evidence that the plume exhibits near self-similar mean profiles of velocity despite the imposed cross-flow. Additionally, Papps & Wood (1997) consider multiple axisymmetric buoyant jets in a cross-flow which merge to form a planar plume in a cross-flow. For this geometry an intermittent flapping motion was observed, increasing the spreading rate of the plume compared with axisymmetric buoyant jets.

Our focus is on a co-flowing environment of steady and uniform vertical velocity w_a and constant density ρ_a. As such, a planar plume in quiescent surroundings ($w_a \equiv 0$) provides a reference case against which the role of the co-flow, that we establish in §§ 3–5, is readily assessed. Pertinent to this reference case is the work of Lee & Emmons (1961) who developed and solved the conservation equations for a turbulent plume from a line source in quiescent surroundings and performed complementary experiments using a thermal plume in air from a source of high aspect ratio ($AR = 138$). For the idealised case of a line source of buoyancy, the power-law solutions based on a constant entrainment coefficient indicate that the mean plume width scales as $b(z) \propto z$, vertical velocity as $w(z) \propto z^0$, and buoyancy as $g'(z) \propto z^{-1}$, where

$$g'(z) = g\frac{\rho_a - \rho(z)}{\rho_a}, \tag{1.1}$$

z denotes the streamwise distance from the source, $\rho(z)$ is the local density of the plume and g the acceleration due to gravity. Focusing on planar plumes from area sources, $b(z = 0) = b_0 > 0$, van den Bremer & Hunt (2014) adopt a variable entrainment model and examine theoretically the behaviour of forced and lazy releases. They consider both Boussinesq and non-Boussinesq cases and following the approach proposed by Hunt & Kaye (2005), in which the conservation equations are re-cast in terms of the local Richardson number $\Gamma(z)$, derive analytical solutions for the primary plume quantities of interest. In §§ 3 and 4 we confirm that our solutions reduce to theirs on setting $w_a = 0$.

A second reference case is that of a turbulent jet issuing from a planar source into a co-flow. Given the densities of the jet and environment are identical, this represents the limiting case for which the buoyancy force is zero. The behaviour of these jets has been the subject of experimental and theoretical study (Hill 1965; Bradbury & Riley 1967; Gaskin

& Wood [2001]). Hill ([1965]) assumes self-preserving velocity profiles and successfully predicts the approximate velocity field using free jet data for $U_0/(U_c - U_0) < 1$, where U_0 is the free-stream velocity and U_c is the jet centreline velocity. In the near-field region of a strong planar jet in a weak co-flow, i.e. where the jet velocity $w_j \gg w_a$, Bradbury & Riley ([1967]) use dimensional arguments to show that the jet width scales as $b_j \propto z$. Moreover, in the region where $w_j \sim w_a$ they show that $b_j \propto z^{1/2}$, confirming both scalings experimentally. To allow for the difference in entrainment between what they refer to as a strong jet and a weak jet, in their theoretical treatment, Gaskin & Wood ([2001]) introduce an entrainment function that is proportional to the co-flow momentum and predict mean quantities that are in agreement with the experimental measurements of Bradbury & Riley ([1967]).

Given the dearth of information concerning planar plumes, it has proven informative to appeal to the literature on axisymmetric plumes in order to ascertain the primary qualitative influence of a co-flow. These studies characterise the strength of the co-flow relative to the plume by means of the velocity ratio

$$\Omega_0 = \frac{w_a}{w_{p0}}, \tag{1.2}$$

where w_{p0} is a characteristic vertical velocity of the plume at the source. In order to distinguish between the co-flow velocity w_a and the dimensionless co-flow velocity Ω_0, hereafter we refer to the latter as the strength of the co-flow.

Subbarao & Cantwell ([1992]) investigate the streamwise transition, from laminar flow to turbulence, of a buoyant helium jet from a circular source in a co-flow of strength $\Omega_0 = 0.5$ (no explicit measure of the background turbulence is given). They reason that the underlying instability observed in experiment is an inviscid, buoyancy-driven phenomenon and suggest the co-flow imposes an 'unusual' degree of regularity on the jet by eliminating random meandering.

For laminar axisymmetric thermal plumes, Riley & Tveitereid ([1984]) perform a linear stability analysis, encompassing co-flow strengths in the range $0 < \Omega_0 < 5$. On dimensional grounds they adopt a characteristic plume velocity of the form $w_{p0} = f(E, c_p, \nu, \rho, g, \phi)$, where E denotes the source heat flux, c_p the specific heat capacity, ν the kinematic viscosity and ϕ the coefficient of cubical expansion. Their investigation was motivated by the experimental observation of the stabilising effect of a co-flow on a laminar plume, although they do not state whose observation. Their analysis confirmed that the co-flow increases the stability of the plume, producing a flattening of the cross-stream vertical velocity profile combined with a reduction in the temperature difference across the plume.

Evidently then, even a basic understanding of the consequences of the coupling between a co-flowing environment and the local behaviour of a planar plume is absent. While the study of stratified quiescent environments has meant that the transfer of buoyancy between environment and plume has been examined in depth (see the review of Kaye [2008]), the same cannot be stated for exchanges of momentum between an environment co-flowing with a plume. This paper aims to bridge this gap by modelling the interaction of a planar plume with a steady co-flowing stream and thereby offering insights into how the dynamical behaviour of the plume adjusts in response to exchanges with its environment.

In § 2 our theoretical model is presented. At the outset we derive conservation equations appropriate for a planar plume in a co-flow and establish that the local behaviour of the plume is characterised by two dimensionless parameters: the scaled source Richardson number, Γ_0, and the ratio of the co-flow and plume source velocities, Ω_0. We limit our model to situations where the plume is entraining, as opposed to situations where fluid is

detrained from the plume. For the latter, detrained fluid is expected to form a buoyant shell around the main plume, fundamentally altering the underlying physics from the case we consider. As § 2 demonstrates, this focus on entraining plumes corresponds to restricting our attention to flows for which the plume velocity $w > w_a$.

The remainder of the paper is laid out as follows. After developing the governing equations in § 2, an expression for the variation of streamwise plume velocity with local Richardson number is derived that holds irrespective of the source conditions. In § 3 the far-field asymptotic behaviour of the plume is investigated. Assuming the plume is dynamically invariant in the far field, the asymptotic velocity and growth rate are deduced. A notable consequence of plume–co-flow interaction is then presented. Specifically, the asymptotic value of the plume Richardson number, $\Gamma = \Gamma_f$, is not a universal constant as it is for quiescent surroundings, where $\Gamma_f \rightarrow 1$ irrespective of the source value Γ_0, but varies with both Ω_0 and Γ_0. These results are then used to extend the work of Rajaratnam & Lal (1983) on a plume from a line source in a co-flow, enabling explicit analytical solutions for the width, vertical velocity and buoyancy to be developed. In § 4 we examine the streamwise development of the plume, including its dynamical variability. For a pure plume release, our solutions show that the co-flow can cause the plume width to linearly decrease or induce necking, the latter giving the flow the appearance of a conventional contracting lazy plume. Indeed, whilst for a quiescent environment the convergence of the plume perimeter to a neck ($\mathrm{d}b/\mathrm{d}z = 0$) is characteristic to lazy releases only, we show that the co-flow may cause a neck to form for forced releases. In § 5 analytical solutions for highly forced ($\Gamma_0 \ll 1$) and highly lazy ($\Gamma_0 \gg 1$) plumes in a weak co-flow ($w_a/w \ll 1$) are presented for the dimensionless streamwise variation of plume velocity, width and Richardson number. Our conclusions are drawn in § 6.

2. Theoretical modelling

The physical situation considered concerns a steady release of buoyant fluid with vertical velocity w_0 and density ρ_0 from a slender rectangular source of width b_0 and infinite length, figure 1. The plume formed by this release issues into an unbounded environment of uniform density ρ_a. The plume is assumed to be fully turbulent so that its flow is independent of the Reynolds number and, as such, the effects of molecular diffusion and viscous effects are negligible. The process of entrainment into this turbulent flow gives rise to a horizontal entrainment velocity, u_e, across the plume perimeter. The environment flows smoothly with a uniform vertical velocity w_a ($=$ const.) such that the plume and its environment are co-flowing, i.e. $\mathrm{sgn}(w_0) = \mathrm{sgn}(w_a)$. The flow of the plume and environment are assumed to be incompressible. Following Morton *et al.* (1956), we make the standard modelling assumptions for the plume. We consider mean quantities, i.e. those spatially averaged along the length of the plume (into the page, figure 1) and in time. Denoting the mean local density of the plume as ρ, we restrict our analysis to density differences between the plume and the environment that are small relative to a reference density, i.e. we make the Boussinesq approximation, whereby $\rho - \rho_a \ll \rho_a$. Accordingly, the buoyancy of the release at the source is $g_0' = g(\rho_a - \rho_0)/\rho_a$. Denoting the local mean plume width as b and vertical velocity as w, the mean fluxes of volume Q, (specific) momentum M and buoyancy B per unit length of the source are thus

$$Q = \int_{-\infty}^{\infty} w \, \mathrm{d}x, \quad M = \int_{-\infty}^{\infty} w^2 \, \mathrm{d}x \quad \text{and} \quad B = \int_{-\infty}^{\infty} w g' \, \mathrm{d}x. \qquad (2.1a\text{--}c)$$

In terms of the fluxes (2.1a–c), the source conditions for the release are

$$Q = Q_0, \quad M = M_0, \quad B = B_0 \text{ on } z = 0. \qquad (2.2a\text{--}c)$$

2.1. *Conservation equations for a planar plume in a co-flow*

In quiescent surroundings, measurements show that the bell-shaped cross-stream profiles of velocity and buoyancy are self-similar and well represented by Gaussians (Rouse, Yih & Humphreys 1952; Lee & Emmons 1961; Chen & Rodi 1980). However, Riley & Tveitereid (1984) note that a co-flow flattens the velocity profile. A long-standing and proven approach for modelling plumes in a wide range of settings has been to make the simplifying assumption that the profiles are top hats. As such, and without clear justification to choose otherwise, we too adopt this simplification. It is readily shown (Appendix A) that the respective equations for the conservation of mass, momentum and buoyancy may then be written

$$\frac{d}{dz}[bw] = 2u_e, \quad \frac{d}{dz}[bw^2] = bg' + 2w_a u_e \quad \text{and} \quad \frac{d}{dz}[bwg'] = 0, \quad (2.3a\text{--}c)$$

where it is clear that the co-flow, manifesting as the second term in (2.3*b*), serves to transport momentum into an entraining plume ($u_e > 0$ signifies flow from the environment across the plume perimeter). To close this system of differential equations, the classic entrainment assumption as proposed by Taylor (1945) is adopted. Accordingly, the horizontal velocity at the plume perimeter is assumed to be directly proportional to a characteristic vertical velocity, in this case, that of the plume relative to the co-flow. Thus,

$$u_e = \alpha(w - w_a), \quad (2.4)$$

where $\alpha(> 0)$ is the entrainment coefficient.

In his discussion on the development of the entrainment assumption, Turner (1986) affirms that even the simplest assumption of a constant entrainment coefficient is surprising in its ability to accurately predict flow behaviours over a wide range of problems and scales. Indeed in quiescent surroundings, the treatment of pure (Morton *et al.* 1956), forced (Morton 1959) and lazy plumes (Hunt & Kaye 2005) by means of a constant entrainment coefficient has offered much insight. Following in this spirit, we also assume $\alpha = \text{const.}$ in our simplified treatment of a plume in a co-flow. While we acknowledge that measurements from one of the earliest studies of planar plumes, namely Rouse *et al.* (1952), suggest a Gaussian entrainment coefficient of $\alpha_G = 0.16$, a number of other measurements support a value closer to 0.10. For example, Ramaprian & Chandrasekhara (1989) report $\alpha_G = 0.11$; both Yuan & Cox (1996) and Paillat & Kaminski (2014) report $\alpha_G = 0.126$; and Parker *et al.* (2020) report $\alpha_G = 0.10$. Given that $\alpha = \sqrt{2}\alpha_G$, a top-hat entrainment coefficient of $\alpha = 0.14$ would not appear to be unreasonable for use in a simplified model. For information on variable entrainment coefficients, the reader is referred to Kotsovinos & List (1977) and van den Bremer & Hunt (2014).

Substituting for $u_e = \alpha(w - w_a)$ into (2.3) gives

$$\frac{d}{dz}[bw] = 2\alpha(w - w_a), \quad \frac{d}{dz}[bw^2] = bg' + 2\alpha(w - w_a)w_a \quad \text{and} \quad \frac{d}{dz}[bwg'] = 0.$$
$$(2.5a\text{--}c)$$

In our framework, $\alpha w_a > 0$ and so the role of a general co-flow is now clear: the momentum flux increases locally if the term $(w - w_a)$ is positive and decreases if $(w - w_a)$ is negative. From the statement of volume conservation in (2.5*a–c*), $(w - w_a) < 0$ corresponds to a detrainment of fluid from the plume. Detrained fluid likely remains in the proximity of the plume perimeter, thereby altering the density of the environment through which the plume propagates. As such, we restrict our attention to releases that entrain fluid, i.e. to co-flows for which $(w - w_a) > 0$. Evaluating the

integrals in (2.1*a–c*), the respective fluxes per unit length of volume, specific momentum and buoyancy for top-hat profiles are

$$Q = bw, \quad M = bw^2 \quad \text{and} \quad B = bwg'. \tag{2.6a–c}$$

Accordingly, (2.5*a–c*) reduces to

$$\frac{\mathrm{d}Q}{\mathrm{d}z} = 2\alpha \left[\frac{M}{Q} - w_a \right], \quad \frac{\mathrm{d}M}{\mathrm{d}z} = \frac{BQ}{M} + 2\alpha \left[\frac{M}{Q} - w_a \right] w_a, \quad \frac{\mathrm{d}B}{\mathrm{d}z} = 0. \tag{2.7a–c}$$

Scaling quantities on the source conditions, we introduce

$$\hat{Q} = \frac{Q}{Q_0}, \quad \hat{M} = \frac{M}{M_0}, \quad \hat{B} = \frac{B}{B_0}, \quad \zeta = \frac{\alpha z}{b_0}, \quad \Omega_0 = \frac{w_a}{w_0}, \tag{2.8a–d}$$

and define the source Richardson number as

$$\Gamma_0 = \frac{B_0 Q_0^3}{2\alpha M_0^3}. \tag{2.9}$$

With reference to § 1, note that $w_{p0} = w_0$ in our definition (2.8*a–d*) of the co-flow strength Ω_0. From (2.7*c*), the buoyancy flux is invariant and in dimensionless form $\hat{B} = 1$. As previously established, in quiescent surroundings $\Gamma_0 = 1$ corresponds to a pure plume release, $\Gamma_0 < 1$ to forced releases and $\Gamma_0 > 1$ to lazy releases (e.g. van den Bremer & Hunt 2014). In terms of the dimensionless quantities (2.8*a–d*) and (2.9), the equations in (2.7) become

$$\frac{\mathrm{d}\hat{Q}}{\mathrm{d}\zeta} = 2 \left[\frac{\hat{M}}{\hat{Q}} - \Omega_0 \right], \quad \frac{\mathrm{d}\hat{M}}{\mathrm{d}\zeta} = 2\Gamma_0 \frac{\hat{B}\hat{Q}}{\hat{M}} + 2 \left[\frac{\hat{M}}{\hat{Q}} - \Omega_0 \right] \Omega_0, \quad \frac{\mathrm{d}\hat{B}}{\mathrm{d}\zeta} = 0. \tag{2.10a–c}$$

As required, (2.10*a–c*) reduces to the governing equations for a planar plume in quiescent surroundings (Lee & Emmons 1961) on setting $\Omega_0 = 0$. As defined, the Richardson number and co-flow strength arise naturally through the non-dimensionalisation of the governing equations.

2.2. *Change of variable: Γ-based approach*

The local Richardson number

$$\Gamma = \frac{BQ^3}{2\alpha M^3} = \frac{bg'}{2\alpha w^2}, \tag{2.11}$$

may be interpreted as a ratio of the local mass, momentum and buoyancy fluxes and, thereby, offers direct insight into the local dynamical behaviour of the plume. For example, if Γ decreases in the streamwise direction, as observed in our results in § 4, this trend signifies that the role of the momentum flux is increasing relative to the buoyancy flux. Moreover, based on the value of Γ relative to unity, the plume may be classified locally as forced, pure or lazy. In their study of planar plumes in quiescent surroundings, van den Bremer & Hunt (2014) adopt the approach developed by Hunt & Kaye (2005) whereby the conservation equations are recast in terms of Γ, the objective of this change of variable

being to enable the dynamical variability to be solved for directly. Following this approach, we first note that

$$\frac{\mathrm{d}\Gamma}{\mathrm{d}z} = \frac{1}{2\alpha}\left[\frac{Q^3}{M^3}\frac{\mathrm{d}B}{\mathrm{d}z} - \frac{3BQ^3}{M^4}\frac{\mathrm{d}M}{\mathrm{d}z} + \frac{3BQ^2}{M^3}\frac{\mathrm{d}Q}{\mathrm{d}z}\right]. \tag{2.12}$$

Substituting for $\mathrm{d}B/\mathrm{d}z$, $\mathrm{d}M/\mathrm{d}z$ and $\mathrm{d}Q/\mathrm{d}z$ from (2.7) into (2.12) and introducing the dimensionless plume width and velocity as

$$\beta = \frac{b}{b_0} \quad \text{and} \quad \omega = \frac{w}{w_0}, \tag{2.13a,b}$$

respectively, yields the required differential equation governing the streamwise variation of Γ, (2.14a). Similar manipulation of the two remaining conservation equations, (2.7a) and (2.7b), yields the associated differential equations for the streamwise variation of β and ω

$$\frac{\mathrm{d}\Gamma}{\mathrm{d}\zeta} = 6\frac{\Gamma}{\beta}\left[1 - \Gamma - 2\frac{\Omega_0}{\omega} + \left(\frac{\Omega_0}{\omega}\right)^2\right], \tag{2.14a}$$

$$\frac{\mathrm{d}\beta}{\mathrm{d}\zeta} = 2\left[2 - \Gamma - 3\frac{\Omega_0}{\omega} + \left(\frac{\Omega_0}{\omega}\right)^2\right], \tag{2.14b}$$

$$\frac{\mathrm{d}\omega}{\mathrm{d}\zeta} = 2\frac{\omega}{\beta}\left[\Gamma - 1 + 2\frac{\Omega_0}{\omega} - \left(\frac{\Omega_0}{\omega}\right)^2\right]. \tag{2.14c}$$

The dimensionless source conditions become

$$\Gamma = \Gamma_0, \quad \beta = 1, \quad \omega = 1 \text{ on } \zeta = 0. \tag{2.15a–c}$$

On setting $\Omega_0 = 0$, (2.14) reduce to the governing equations derived by van den Bremer & Hunt (2014) − the sole differences are factors of two which result from our scaling being based on the full width of the plume, rather than the half-width. For the purpose of reference the solutions for a quiescent environment ($\Omega_0 = 0$) are given in Appendix C.

To solve for the streamwise velocity, dividing (2.14a) by (2.14c) yields $\mathrm{d}\Gamma/\mathrm{d}\omega = -3\Gamma/\omega$, which may be integrated straightforwardly to give

$$\omega = \left(\frac{\Gamma_0}{\Gamma}\right)^{1/3}. \tag{2.16}$$

The corresponding solutions of (2.14a)–(2.14c) for Γ and β are dealt with in § 4. Whilst Ω_0 does not appear explicitly in (2.16), whose forms appears identical to the solution derived for the $\Omega_0 = 0$ case (Appendix C), the effect of a co-flow is to modify the variation of $\Gamma(\zeta)$ relative to the $\Omega_0 = 0$ case.

3. Asymptotic solutions

Prior to investigating the near-source behaviour (§§ 4 and 5), we examine the effect of Γ_0 and Ω_0 on the far-field behaviour of plumes from sources of finite width and develop solutions for the plume from an idealised line source in § 3.4.

932 A41-8

3.1. *Asymptotic velocity ω_f*

In the far field, Γ remains positive and it is expected that $\mathrm{d}\Gamma/\mathrm{d}\zeta \to 0$, i.e. the plume approaches a dynamically invariant behaviour. Thus, while (2.14*b*) and (2.14*c*) are unchanged, (2.14*a*) reduces to

$$0 = 1 - \Gamma - 2\frac{\Omega_0}{\omega} + \frac{\Omega_0^2}{\omega^2}. \tag{3.1}$$

Substituting (3.1) into (2.14*c*) gives

$$\frac{\mathrm{d}\omega}{\mathrm{d}\zeta} = 0 \implies \omega = \omega_f = \text{const.,} \tag{3.2}$$

where the subscript f is used to denote the far-field value of a quantity. On physical grounds $\omega_f > 0$ as the plume and the environment are co-flowing. Substituting (2.16) into (3.1) leads to the following cubic polynomial in ω_f:

$$\omega_f^3 - 2\Omega_0\omega_f^2 + \Omega_0^2\omega_f - \Gamma_0 = 0, \tag{3.3}$$

whose discriminant can be written as

$$\Delta = \Gamma_0(4\Omega_0^3 - 27\Gamma_0). \tag{3.4}$$

The asymptotic velocity is, in general, not equal to the co-flow velocity. Indeed, these velocities are equal only for a true jet ($\Gamma_0 = 0$), as is readily confirmed on substituting $\omega_f = \Omega_0$ into (3.3). With $k \in \{0, 1, 2\}$ and defining the constant C_k as

$$C_k = \frac{1}{\sqrt[3]{2}}\sqrt[3]{(2\Omega_0^3 - 27\Gamma_0 - \sqrt{\Gamma_0(729\Gamma_0 - 108\Omega_0^3)})}\left(\frac{-1+\sqrt{-3}}{2}\right)^k, \tag{3.5}$$

where $\sqrt[3]{()}$ indicates the principal root, the roots of (3.3) are

$$\omega_f = \frac{1}{3}\left(2\Omega_0 - C_k - \frac{\Omega_0^2}{C_k}\right). \tag{3.6}$$

For $\Gamma_0 > 4\Omega_0^3/27$, (3.3) has one real-valued root as the discriminant is strictly negative. Moreover, this root is positive as may be reasoned as follows: the curve $y = \omega_f^3 - 2\Omega_0\omega_f^2 + \Omega_0^2\omega_f - \Gamma_0$ intersects the ordinate at $y = -\Gamma_0$ and, as there is a single real root and $\lim_{w_f \to +\infty}(y) = +\infty$, the curve must intersect the abscissa once, at a positive value of w_f. The other two roots are complex conjugates and are therefore discounted on physical grounds, leaving a single admissible root for the far-field velocity. In this case, the valid root is obtained on setting $k = 1$. Noting that the local co-flow strength Ω can be expressed as

$$\Omega = \Omega_0/\omega, \tag{3.7}$$

figure 2 plots the direction of the vector $\{\mathrm{d}\Gamma/\mathrm{d}\zeta, \mathrm{d}\Omega/\mathrm{d}\zeta\}$ in (Γ, Ω) space. This vector plot demonstrates that the stable solutions of (3.3) are those for which $\Omega = \Omega_0/\omega < 1$ as, in this region, the vectors point towards these solutions.

For $\Gamma_0 < 4\Omega_0^3/27$, there are three real-valued roots which, by Descartes sign theorem, may all be positive. The valid root in this case is identified by insisting $\Omega_0/w_f \leq 1$ (equivalently $(w_f - w_a) \geq 0$), i.e. that there is no detrainment, which figure 2 demonstrates
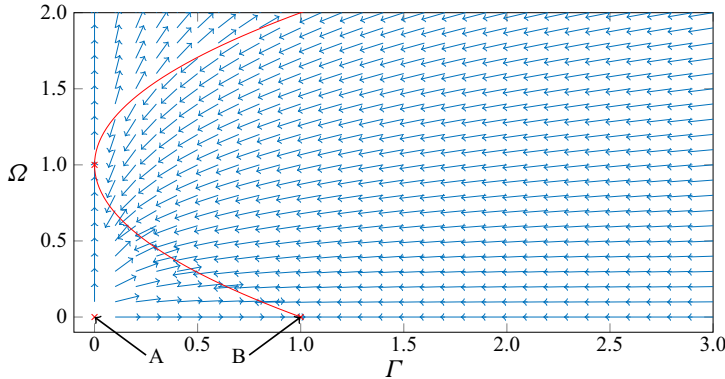
Figure 2. Vector plot showing the direction of the vector $\{d\Gamma/d\zeta, d\Omega/d\zeta\}$ in (Γ, Ω) space. Locations where $d\Gamma/d\zeta = d\Omega/d\zeta = 0$ are shown in red. These locations are $(0,0)$, $(1,0)$, $(0,1)$ and points satisfying the equation $\Gamma = \Omega^2 - 2\Omega + 1$ as shown by the red curve. Vectors have been normalised by their magnitude so as to aid interpretation of the plot.
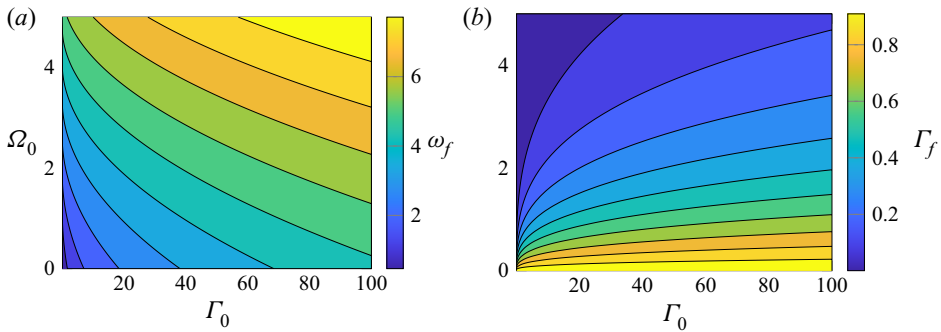

Figure 3. Variation of asymptotic vertical velocity and Richardson number with Γ_0 and Ω_0. (*a*) Contours of constant ω_f with colour bar indicating the magnitude of ω_f. (*b*) Contours of constant Γ_f with colour bar indicating the magnitude of Γ_f.

is a necessary condition for a stable solution in the far field. In this case, the valid root is obtained on setting $k = 2$.

Point A at $(\Gamma_0 = 0, \Omega = \Omega_0 = 0)$ in figure 2 marks the classic jet solution for which any incremental increase in the buoyancy of the release (corresponding to an increase in Γ) or co-flow strength (corresponding to an increase in Ω) drives the flow away from this unstable solution. The stable classic pure plume solution at Point B $(\Gamma_0 = 1, \Omega = \Omega_0 = 0)$ and all points along the red curve, which plots $\Gamma = \Omega^2 - 2\Omega + 1$ from (3.1), are the coordinates in (Γ, Ω) space where $d\Gamma/d\zeta = d\Omega/d\zeta = 0$. Note that for $\Omega = \Omega_0/\omega \leq 1$ the arrows point towards the curve, indicating that those solutions are stable.

3.2. *Asymptotic growth rate*

Subtracting (3.1) from (2.14*b*) gives

$$\frac{d\beta}{d\zeta} = 2\left(1 - \frac{\Omega_0}{\omega_f}\right) = \text{const.}, \tag{3.8}$$

and, hence, the relative asymptotic growth rates in co-flowing and quiescent environments are

$$\frac{\mathrm{d}\beta}{\mathrm{d}\zeta} \bigg/ \frac{\mathrm{d}\beta}{\mathrm{d}\zeta}\bigg|_{\Omega_0=0} = 1 - \frac{\Omega_0}{\omega_f}. \tag{3.9}$$

For the reference case of a zero co-flow, (3.8) reduces to the positive growth rate $\mathrm{d}\beta/\mathrm{d}\zeta = 2$ in accordance with the predictions of Lee & Emmons (1961) and van den Bremer & Hunt (2014). Integrating (3.8) gives the far-field width as

$$\beta = \frac{b}{b_0} = f(\zeta) + 2\zeta - 2\frac{\Omega_0}{\omega_f}\zeta, \tag{3.10}$$

with $f(0) = 1$ and $f(\zeta) \to C = \mathrm{const.}$ for $\zeta \to \infty$. While presented here as an asymptotic solution, (3.10) is valid for all ζ for the special case of a linearly expanding plume (analogous to a pure release in zero co-flow). Further consideration of this special case (§ 4.2) offers additional insight into the role of the co-flow. Given Ω_0 and ω_f are positive constants, $\Omega_0/\omega_f > 0$, and it is clear that the third term in (3.10) acts to reduce the plumes width, cf. the expression for β in (C 1).

3.2.1. *The case $\Omega_0/\omega_f > 1$*
Equation (3.8) shows that $\mathrm{d}\beta/\mathrm{d}\zeta$ is negative in the far field and, thus, the plume contracts. Given $\Omega_0/\omega_f > 1$ is equivalent to $(w - w_a) < 1$, this reduction in width is due to detrainment. This detrainment causes the plume width to reduce to zero, (3.10), implying a contradiction of the current model and is not considered further.

3.2.2. *The case $\Omega_0/\omega_f = 1$*
From (3.10), $\mathrm{d}\beta/\mathrm{d}\zeta = 0$ and hence the asymptote has constant width. Substitution of $\Omega_0/\omega_f = 1$ into (2.14b) shows that this far-field solution requires $\Gamma_0 = 0$. Furthermore, setting $\Gamma_0 = 0$ and $\Omega_0/\omega_f = 1$ in (2.14a) shows that $\mathrm{d}\Gamma/\mathrm{d}\zeta = 0 \implies \Gamma(\zeta) = \Gamma_0$, i.e. the flow is dynamically invariant. From (2.16), $\omega = (\Gamma_0/\Gamma)^{1/3} = 1$ and thus $\Omega_0 = 1$. In other words, it is only possible for the release and co-flow to have an identical velocity in the far field ($\Omega_0/\omega_f = 1$) for a non-buoyant release into a co-flow with an identical velocity, i.e. $w_0 = w_a$, the release simply forming a continuation of the co-flowing environment.

3.2.3. *The case $0 < \Omega_0/\omega_f < 1$*
The plume expands, although at a reduced rate than in quiescent surroundings, see (3.9). The resulting linearly increasing width and constant vertical velocity asymptotes, (3.2), are consistent with the far-field scalings of Rajaratnam & Lal (1983). The flows that lead to the far-field behaviours $0 < \Omega_0/\omega_f < 1$ form the focus of the remainder of this paper.

3.3. *Asymptotic Richardson number*
The far-field Richardson number $\Gamma = \Gamma_f$ is obtained on substitution of ω_f from (3.6) into (2.16)

$$\Gamma_f = \frac{\Gamma_0}{\omega_f^3} = 27\Gamma_0 \left(2\Omega_0 - C_k - \frac{\Omega_0^2}{C_k}\right)^{-3} \quad \text{where } k = \begin{cases} 1, & \text{if } \Gamma_0 > 4\Omega_0^3/27 \\ 2, & \text{if } \Gamma_0 < 4\Omega_0^3/27. \end{cases} \tag{3.11}$$

The variation of the far-field velocity (3.6) and Richardson number (3.11) with Γ_0 and Ω_0 is shown on the contour plots in figure 3. It is apparent that the velocity in the far field

ω_f increases as either the strength of the co-flow or source Richardson number increases (figure 3a).

On the abscissa $\Omega_0 = 0$ of figure 3(b), $\Gamma_f = 1$ irrespective of the source Richardson number as was to be expected based on existing results for plumes in quiescent surroundings. Clearly, the effect of the co-flow is to reduce the far-field value of Γ_f relative to the reference case of a zero co-flow. In other words, the co-flow increases the 'forced-ness' of the far-field plume.

3.4. *Power-law solutions for a line source*

On dimensional grounds, power-law solutions for the plume that develops from a line source take the form

$$w - w_a = c_1, \quad b = c_2 z, \quad g' = c_3 z^{-1}, \qquad (3.12a\text{--}c)$$

for the unknown coefficients c_1, c_2 and c_3. Rajaratnam & Lal (1983) provide implicit relationships for the coefficients and comment that if the value of one is known, say from experiment, then the other two may be determined. We show below how each coefficient can be determined explicitly with reference to the results developed above.

Substituting for $w = w_f$ from (3.6) into (3.12a–c) leads to

$$c_1 = w_0(\omega_f - \Omega_0) = -\frac{w_0}{3}\left(\Omega_0 + C_k + \frac{\Omega_0^2}{C_k}\right). \qquad (3.13)$$

Substituting for $\zeta = \alpha z / b_0$ in (3.10) gives

$$b = b_0 f(\zeta) + 2\alpha\left(1 - \frac{\Omega_0}{\omega_f}\right)z. \qquad (3.14)$$

Asymptotically far from the source, the first term in (3.14) is diminishingly small relative to the second, and, hence, equating (3.14) with $b = c_2 z$ from (3.12a–c) gives

$$c_2 = 2\alpha\left(1 - \frac{\Omega_0}{\omega_f}\right). \qquad (3.15)$$

In the far field, $\Gamma = \Gamma_f = \Gamma_0/\omega_f^3$ from (2.16) and $b = 2\alpha(1 - \Omega_0/\omega_f)z$ from (3.14). Thus, given $g' = 2\alpha w^2 \Gamma/b$ from (2.11), the buoyancy in the far field may be written as $g' = c_3 z^{-1}$ where

$$c_3 = \frac{\Gamma_0 w_0^2}{\left(1 - \dfrac{\Omega_0}{\omega_f}\right)\omega_f}. \qquad (3.16)$$

As an aside, we note from (3.13) that $c_1/w_0 = (1 - \Omega_0/\omega_f)\omega_f$ and, hence, $c_3 = \Gamma_0 w_0^3/c_1$. The variation of the non-dimensional coefficients $k_1 = c_1/w_0$, $k_2 = c_2/\alpha$ and $k_3 = c_3/w_0^2$ with the co-flow strength and source Richardson number are plotted in figure 4. As expected, for $\Gamma_0 = 1$ and $\Omega_0 = 0$, $k_1 = 1$, i.e. the vertical velocity above a line source is invariant.
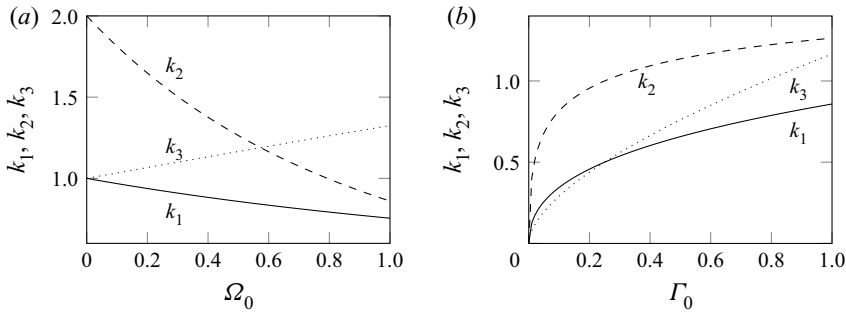
932 A41-12

Figure 4. The variation of the non-dimensional coefficients $k_1 = c_1/w_0$, $k_2 = c_2/\alpha$ and $k_3 = c_3/w_0^2$ with (*a*) Ω_0 and (*b*) Γ_0 for the example values of $\Gamma_0 = 1$ and $\Omega_0 = 0.5$, respectively.

4. Streamwise variation for general source conditions

Prior to examining the behaviours that are specific to the individual class of release, namely, forced (§ 4.2), pure (§ 4.3) and lazy (§ 4.4), we first remark on the trends common to all. For each class, figure 5 plots the streamwise variation of plume width and Richardson number for different strengths of co-flow, and figure 6 plots the streamwise variation of the plume velocity ω and dilution g'/g'_0. The solutions shown in these plots were obtained by numerically integrating (2.14) subject to the relevant source conditions. In each subplot, the solid line depicts the reference case of a co-flow with zero velocity. Re-plotted on logarithmic scales in Appendix B, these solutions confirm the anticipated far-field power-law dependencies (Rajaratnam & Lal 1983) and enable an assessment of whether the near-source variations approximate to power laws. As Ω_0 increases, common to each class of release there is:

   (i) a narrowing of the plume relative to the zero co-flow reference case and, for a sufficiently strong co-flow, the formation of a 'neck' at which the width is a minimum; the conditions that result in necking behaviour are determined in § 4.1;
  (ii) a reduction in the asymptotic value of the Richardson number Γ_f as is indicative of a far-field plume with an excess of momentum flux relative to the reference case. For the co-flows of interest, the fluid entrained enhances the vertical gradient of momentum in the plume (2.5*a–c*) and it is therefore not surprising that these co-flows lead to a reduction in Γ_f compared with the reference case. The asymptotic behaviour of Γ relative to the source value Γ_0 is more nuanced, varying with the class of release, and is considered in §§ 4.2–4.4; and
 (iii) a reduction in dilution; the reasons underpinning this characteristic behaviour are discussed below.

Regarding (i) and (ii), a narrowing in width is also a feature shared by plumes subjected to off-source heating (Bhat & Narasimha 1996; Agrawal & Prasad 2004; Hunt & Kaye 2005). The similarity, however, extends no further. By contrast to the far-field 'forced' behaviour in the presence of a co-flow, plumes with off-source heating asymptote to 'lazy' behaviour. Consistent with the resulting streamwise variations in Richardson number, these contrasting dynamical behaviours were to be expected as the co-flow provides 'off-source' momentum rather than buoyancy.

Regarding (iii), given the entrainment velocity $u_e = \alpha(w - w_a)$, an increase in the velocity of the co-flow relative to the plume reduces u_e and, hence, the flow rate entrained into the plume. Thus, the dilution of the buoyancy or a tracer transported by the plume
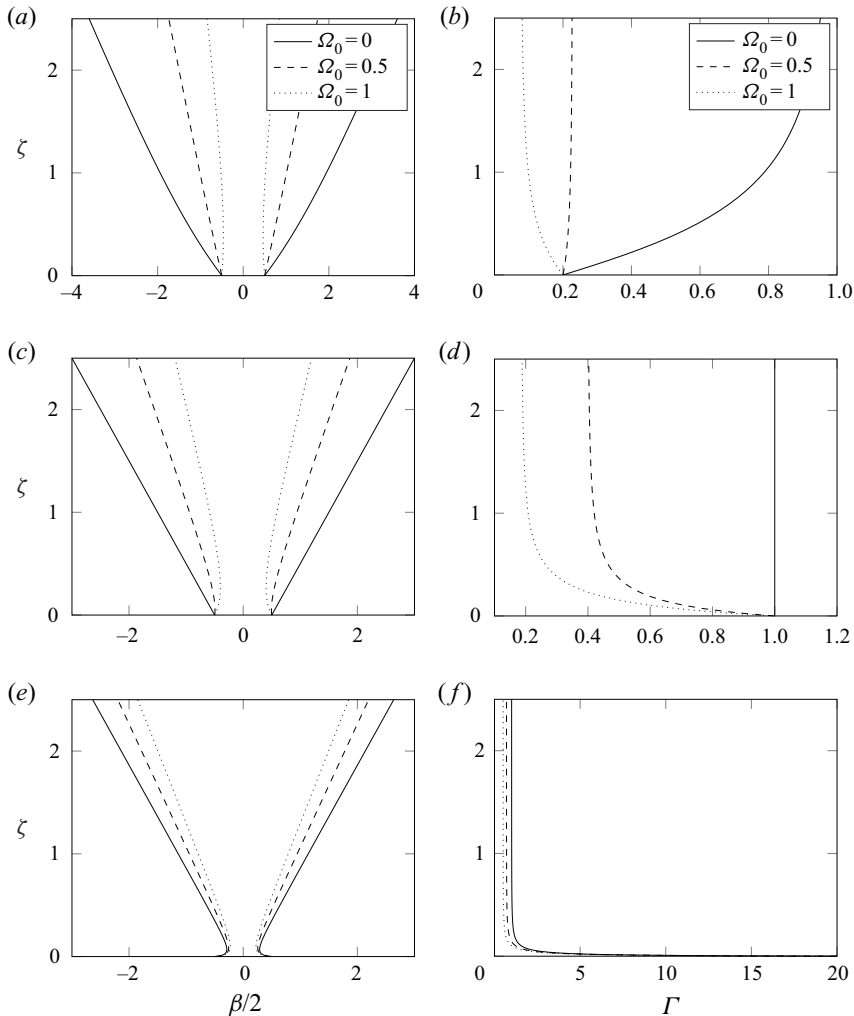
Figure 5. The effect of the co-flows $\Omega_0 = \{0, 0.5, 1\}$ on the streamwise variation of plume width β (left column) and local Richardson number Γ (right column) for (*a–b*) forced ($\Gamma_0 = 0.2$), (*c–d*) pure ($\Gamma_0 = 1$) and (*e–f*) lazy ($\Gamma_0 = 20$) release conditions.

is reduced on account of a co-flowing environment. For a given Ω_0, it is apparent from figure 6 that releases with a greater source Richardson number dilute over a shorter streamwise distance. The trends predicted for the three classes of release are, however, qualitatively similar. This similarity becomes clear with the aid of successively magnified views of the near-source region of figure 6(*f*) (see Appendix D); as this region is magnified, the trends predicted for pure releases (figure 6*d*) and forced releases (figure 6*b*) are immediately apparent.

The co-flow $\Omega_0 = 1$ is unique in that it eliminates the shear between the release and co-flow at the level of the source. A particularly striking feature is apparent for this co-flow, namely, there is almost no dilution of the released fluid in the immediate near-source region. This region of weak dilution, most evident in figure 6(*b*) (see also Appendix D), can be explained by considering the entrainment velocity at, and near, the source. Noting the
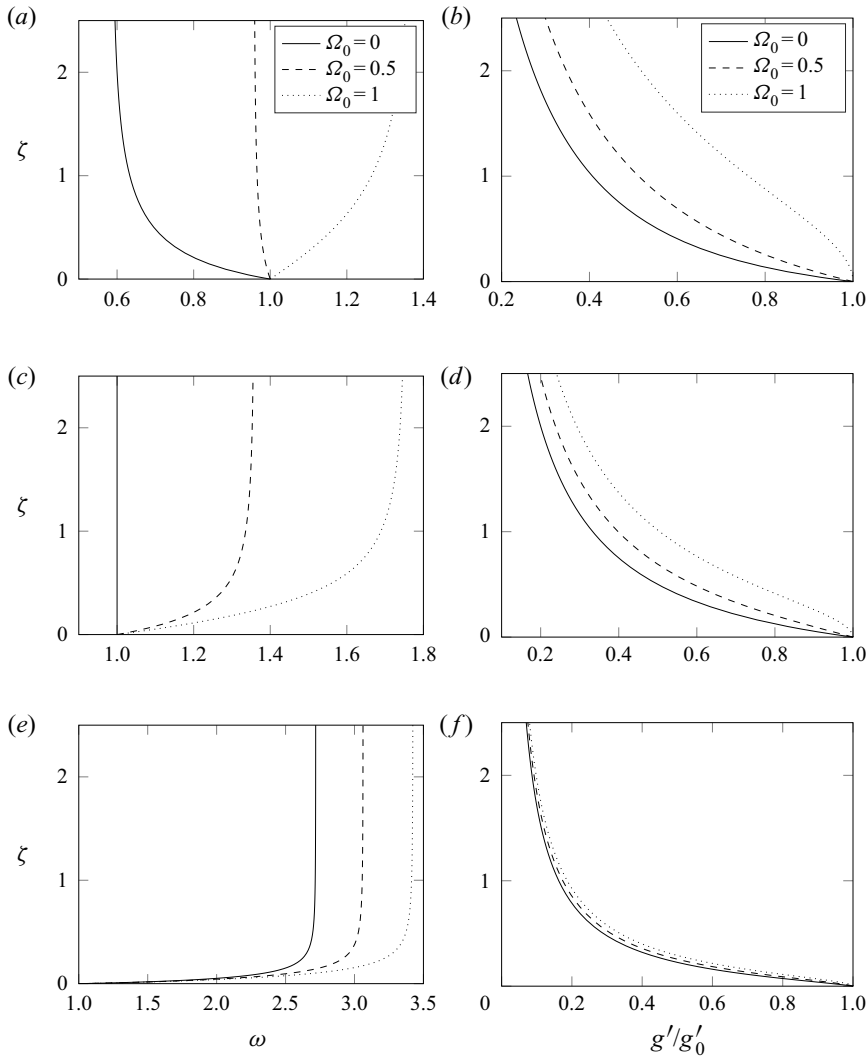
Figure 6. The effect of the co-flows $\Omega_0 = \{0, 0.5, 1\}$ on the streamwise variation of vertical velocity ω (left column) and dilution g'/g'_0 (right column) for (a–b) forced ($\Gamma_0 = 0.2$), (c–d) pure ($\Gamma_0 = 1$) and (e–f) lazy ($\Gamma_0 = 20$) release conditions.

dimensionless entrainment velocity may be expressed as

$$\frac{u_e}{w_a} = \alpha \left(\frac{w}{w_a} - 1 \right) = \alpha \left(\frac{1 - \Omega}{\Omega} \right), \tag{4.1}$$

it is clear that a zero entrainment velocity and, hence, an absence of dilution at the source is unique to the co-flow $\Omega = \Omega_0 = 1$. Given the absence of a velocity differential, the release is entirely buoyancy dominated on entering the co-flow and, thus, contracts ($\mathrm{d}\beta/\mathrm{d}\zeta < 0$) immediately upon release. This contraction is readily confirmed on noting that for $\Omega_0 = 1$, $\Omega_0/\omega|_{\zeta=0} = 1$ and, hence, from (2.14b)

$$\left. \frac{\mathrm{d}\beta}{\mathrm{d}\zeta} \right|_{\zeta=0} = 2 \left[2 - \Gamma - 3\frac{\Omega_0}{\omega} + \left(\frac{\Omega_0}{\omega} \right)^2 \right] \bigg|_{\zeta=0} = -2\Gamma_0 \quad \text{for } \Omega_0 = 1. \tag{4.2}$$

The gradient (4.2) is negative for all $\Gamma_0 \neq 0$. Thus, all releases contract under conditions of no shear at source, while releases with a greater source Richardson number exhibit a more pronounced contraction.

4.1. *Plume contraction*

In the above, plume contraction ($\mathrm{d}\beta/\mathrm{d}\zeta < 0$) has been considered only for the co-flow $\Omega_0 = 1$. Contraction in the absence of a co-flow occurs on account of the streamwise acceleration of the plume when the local Richardson number $\Gamma > 2$ (van den Bremer & Hunt 2014). It is clear from figure 5 that a contraction and the associated necking can also occur for both forced and pure releases for a sufficiently strong co-flow. This behaviour is of particular note as only lazy plumes can exhibit a contraction in the absence of a co-flow. From (2.14*b*), a contraction requires that locally

$$\Gamma > 2 - 3\frac{\Omega_0}{\omega} + \left(\frac{\Omega_0}{\omega}\right)^2. \tag{4.3}$$

As $\zeta \to 0$, $\omega \to 1$ and so a contraction immediately above the source requires

$$\Gamma_0 > 2 - (3\Omega_0 - \Omega_0^2). \tag{4.4}$$

For the co-flows of interest, i.e. $0 < \Omega_0 \leq 1$, $(3\Omega_0 - \Omega_0^2) > 0$ and, hence, a co-flow lowers the threshold source Richardson number above which contraction occurs. For the strongest co-flow considered ($\Omega_0 = 1$) this threshold is $\Gamma_0 > 0$, indicating that contraction would occur irrespective of the class of release. Setting $\Gamma_0 = 1$ reveals that $\Omega_0 = 3/2 - \sqrt{5/4}$ is the minimum co-flow strength which causes a pure release to contract at source.

That the co-flow causes plume contraction at a lower source Richardson number than in quiescent surroundings can be explained by considering the acceleration of the released fluid adjacent to the source. A defining characteristic of a co-flow is the production of a strong positive streamwise velocity gradient in the near-source region for pure and lazy releases (figures 6*c* and 6*e*) a gradient that increases with Ω_0 and decreases downstream. As $\zeta \to 0$, $\beta \to 1$, $\omega \to 1$ and $\Gamma \to \Gamma_0$, and so (2.14*c*) reduces to

$$\left.\frac{\mathrm{d}\omega}{\mathrm{d}\zeta}\right|_{\zeta=0} = 2(\Gamma_0 - 1) + 2(2\Omega_0 - \Omega_0^2). \tag{4.5}$$

Inspection of the second term of (4.5) reveals $2(2\Omega_0 - \Omega_0^2) > 0$ for $0 < \Omega_0 \leq 1$ and that its magnitude increases with Ω_0. Thus, the presence of a co-flow enhances the acceleration of the release and a maximum acceleration occurs for $\Omega_0 = 1$, i.e. for a co-flow that produces no shear at the source. Whether or not the release contracts is determined by the interplay between entrainment (which acts to increase plume width) and acceleration (which, by conservation of mass, acts to decrease plume width). At the source, (2.14*b*) reduces to

$$\left.\frac{\mathrm{d}\beta}{\mathrm{d}\zeta}\right|_{\zeta=0} = 2(2 - \Gamma_0 - 3\Omega_0 + \Omega_0^2), \tag{4.6}$$

which, combined with (4.5) yields

$$\left.\frac{\mathrm{d}\beta}{\mathrm{d}\zeta}\right|_{\zeta=0} = 2(1 - \Omega_0) - \left.\frac{\mathrm{d}\omega}{\mathrm{d}\zeta}\right|_{\zeta=0}. \tag{4.7}$$

Given that $2(1 - \Omega_0) \to 0$ and $\mathrm{d}\omega/\mathrm{d}\zeta|_{\zeta=0}$ increases as $\Omega_0 \to 1$, (4.7) demonstrates that the acceleration dominates the interplay as the co-flow strengthens, leading to $\mathrm{d}\beta/\mathrm{d}\zeta|_{\zeta=0} < 0$, i.e. to plume contraction.

932 A41-16

As a final remark on plume contraction, it is readily shown (Appendix E) that the Richardson number at the neck Γ_n reduces with increasing Ω_0, the magnitude of the reduction decreasing as Γ_0 increases.

4.2. *The case $\Gamma_0 < 1$*

The solutions plotted in figure 5(*a*) show a pronounced reduction in the width of the forced release as the co-flow increases in strength, and the appearance of a local minimum, i.e. of a neck. The accompanying plot, figure 5(*b*) showing the streamwise variation of Γ, reveals the profound influence a co-flow has on the dynamical behaviour. In the absence of a co-flow, Γ increases monotonically towards unity as is well documented. However, for a sufficiently weak co-flow, $\Gamma(\zeta)$ is an increasing function of ζ and leads to $\Gamma_0 < \Gamma_f < 1$. In other words, the relative excess of momentum flux introduced at the source is reduced downstream, where the plume is locally less forced than at the source. By contrast, for both pure and lazy releases into non-zero co-flows, $\Gamma(\zeta)$ decreases towards the far-field value $\Gamma_f < 1$ following similar trends (figures 5*d* and 5*f*). Thus, their far-field behaviour is 'forced', characterised by a relative excess of momentum flux.

Returning to forced releases, given $\mathrm{d}\Gamma/\mathrm{d}\zeta|_{\zeta=0} > 0$ for $\Omega_0 = 0$ and $\mathrm{d}\Gamma/\mathrm{d}\zeta|_{\zeta=0} < 0$ for $\Omega_0 = 1$, see (2.14*a*) and figure 5(*b*) it is natural to enquire whether a particular co-flow strength, $\Omega_0 = \Omega_0^*$, leads to a dynamically invariant plume. From (2.14*a*)

$$\frac{\mathrm{d}\Gamma}{\mathrm{d}\zeta} = 0 \implies 6\frac{\Gamma}{\beta}\left[1 - \Gamma - 2\frac{\Omega_0^*}{\omega} + \left(\frac{\Omega_0^*}{\omega}\right)^2\right] = 0 \implies 1 - \Gamma_0 - 2\frac{\Omega_0^*}{\omega} + \left(\frac{\Omega_0^*}{\omega}\right)^2 = 0,$$
(4.8)

provided $\Gamma/\beta \neq 0$. Insisting $\mathrm{d}\Gamma/\mathrm{d}\zeta = 0$, (2.16) reduces to $\omega = 1$ which on substitution into (4.8) yields the required co-flow, namely

$$\Omega_0^* = 1 \pm \sqrt{\Gamma_0}.$$
(4.9)

In conjunction with a constant plume velocity ω, this co-flow necessarily results in a linearly varying plume width, as is confirmed from (2.14*b*)

$$\frac{\mathrm{d}\beta}{\mathrm{d}\zeta} = \mp 2\sqrt{\Gamma_0} \implies \beta = \mp 2\sqrt{\Gamma_0}\zeta + 1 \quad \text{for } \Omega_0 = \Omega_0^*.$$
(4.10)

Evidently, the smaller root $\Omega_0^* = 1 - \sqrt{\Gamma_0}$ results in a linearly increasing plume width ($\mathrm{d}\beta/\mathrm{d}\zeta > 0$) and the larger root, a linearly decreasing plume width ($\mathrm{d}\beta/\mathrm{d}\zeta < 0$). The larger root $\Omega_0^* = 1 + \sqrt{\Gamma_0}$ necessarily results in detrainment (see (4.1)) and so is not considered further.

4.3. *The case $\Gamma_0 = 1$*

As the sole restriction placed on the derivation of (4.9) is $\Gamma/\beta \neq 0$, the expression for Ω_0^* holds across all three classes of release with the exclusion of the jet ($\Gamma_0 = 0$). For a pure plume release, (4.9) reproduces the classic result that Γ is invariant in a co-flow of zero velocity and provides the new result that the co-flow $\Omega_0 = 2$ causes a pure release to decrease linearly in width until $\beta = 0$, at which point the model breaks down.

As the co-flow strengthens, the plume width reduces markedly (figure 5*c*). The plume outline transitions from straight sided (with $\Omega_0 = 0$) to resembling a lazy plume in quiescent surroundings owing to the appearance of a neck (e.g. with $\Omega_0 = 1$). Moreover, the relative velocity of the plume ($w - w_a$) decreases. Thus in the reference frame of the
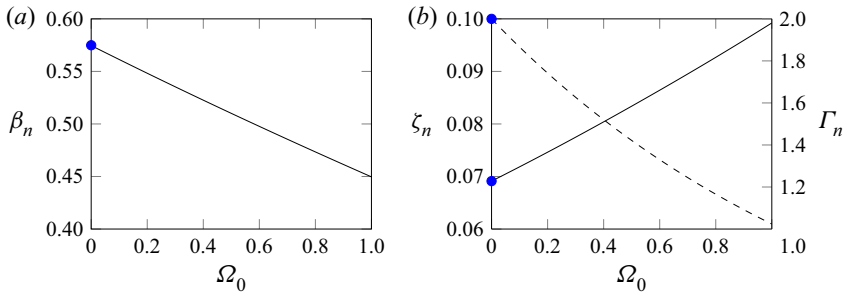
Figure 7. Variation of the plume neck with co-flow strength for the lazy release $\Gamma_0 = 20$; (*a*) β_n vs Ω_0, (*b*) ζ_n vs Ω_0 (solid line), and Γ_n vs Ω_0 (dashed line). Here, ● (blue) show the solutions of van den Bremer & Hunt (2014) for a quiescent environment.

plume, the inertial force decreases and, consequently, the buoyancy force associated with the plume plays an increasingly dominant role – this trend ultimately leading to plume contraction (see § 4.1).

The gradient $d\Gamma/d\zeta$ reveals a strong dynamical variation in the near field of the plume, a variation that increases with Ω_0. Further downstream, the gradient weakens and the subsequent vertical variation is slow as the plume asymptotes to its far-field behaviour (§ 3.3). Notably, the release becomes increasingly forced downstream as the co-flow strengthens.

4.4. *The case $\Gamma_0 > 1$*

In the absence of a co-flow, Γ rapidly converges to unity due to the excess of buoyancy relative to a pure plume (van den Bremer & Hunt 2014). This rapid variation is also evident in the presence of a co-flow (figure 5*f*). Increasing the strength of the co-flow also reduces the plume width, though to a considerably lesser extent than for pure and forced releases. Moreover, the co-flow accentuates the plume neck, which narrows, forms further downstream and at a lower local Richardson number. These trends are shown in figure 7 for the example release $\Gamma_0 = 20$. The location and width of the neck was found numerically by locating the sign change in $d\beta/d\zeta$. The closed-form solution for Γ_n (Appendix E) was derived by substituting (2.16) into (2.14*b*) and setting $d\beta/d\zeta = 0$.

4.5. *Adjustment to locally pure plume behaviour*

To acquire further insight into the role of a co-flow it is informative to examine the streamwise distance over which a release adjusts to locally pure plume conditions. The 'adjustment' length $\zeta_{\Gamma=1}$ over which this dynamical variation occurs is defined such that $\Gamma(\zeta_{\Gamma=1}) = 1$ and, as a consequence, is meaningful only for releases for which $\Gamma_0 > 1$. In quiescent surroundings $\Gamma(\zeta) \rightarrow \Gamma_f = 1$ as $\zeta \rightarrow \infty$ for $\Gamma_0 \neq 1$, i.e. the adjustment length is infinite for $\Gamma_0 > 1$. It is clear, however, that a co-flow significantly alters the behaviour of $\Gamma(\zeta)$, reducing the far-field Richardson number to a value below unity (figure 5). With reference to (2.14*a*)

$$\zeta_{\Gamma=1} = \int_0^{\zeta_{\Gamma=1}} d\zeta = \int_{\Gamma_0}^1 \frac{\beta}{6\Gamma\left(1 - \Gamma - 2\dfrac{\Omega_0}{\omega} + \left(\dfrac{\Omega_0}{\omega}\right)^2\right)} d\Gamma. \qquad (4.11)$$
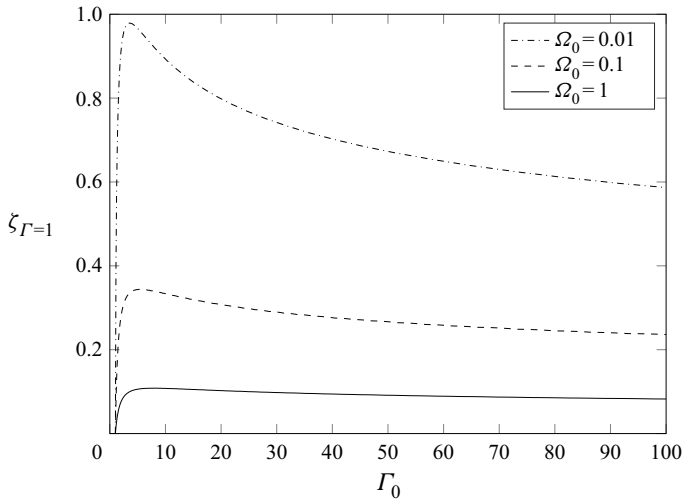
Figure 8. The vertical distance $\zeta_{\Gamma=1}$, (4.11), over which the release adjusts to locally pure plume conditions plotted against Γ_0 for $\Omega_0 = \{0.01, 0.1, 1\}$. The plot cannot be extended to forced releases as these never attain $\Gamma = 1$ for $\Omega_0 \neq 0$. The figure was generated by numerically integrating (2.14) and interpolating to find the height at which $\Gamma = 1$.

Comparing the finite distance (4.11) over which the Richardson number reduces from $\Gamma = \Gamma_0 \, (> 1)$ to $\Gamma = 1$ for different strengths of co-flow allows us to establish whether the inertia of the co-flow or the buoyancy force of the plume is dominant in controlling the dynamical behaviour. Figure 8 plots $\zeta_{\Gamma=1}$ vs Γ_0 for non-zero co-flows that vary by two orders of magnitude. Below each curve the plume is locally lazy (i.e. for $\zeta < \zeta_{\Gamma=1}$), above each curve the plume is locally forced (i.e. for $\zeta > \zeta_{\Gamma=1}$) and on the curves the plume is pure. Evidently, the adjustment to a pure plume state is now attained over a finite distance. Moreover, for $\zeta > \zeta_{\Gamma=1}$ the release continues to adjust such that asymptotically $\Gamma \to \Gamma_f < 1$. As the co-flow increases in strength, $\zeta_{\Gamma=1}$ decreases and the variation of $\zeta_{\Gamma=1}$ with Γ_0 weakens − note the flatness of the curve when $\Omega_0 = 1$. The decrease in $\zeta_{\Gamma=1}$ can be attributed to the increase in momentum transported by the plume as the co-flow strengthens, an increase that acts to reduce Γ, see (2.11).

The weakening variation of $\zeta_{\Gamma=1}$ with Γ_0 as Ω_0 increases is indicative of co-flows having an increasingly dominant influence on plume behaviour. That $\zeta_{\Gamma=1}$ hardly varies with Γ_0 for the co-flow $\Omega_0 = 1$ (figure 8 for $\Gamma_0 \gtrsim 5$) suggests that, as defined, $\Omega_0 = 1$ be regarded as a 'strong' co-flow; this assertion is consistent with this co-flow reducing the shear at the source to zero (§ 4). However, while nuanced, the role of buoyancy on the interaction between co-flow and plume is evident in figure 8; note the decreasing spacing between the three curves as Γ_0 increases, a trend signifying that the influence of a given co-flow on the plume lessens for increasingly buoyancy dominated releases. Indeed, this result is also borne out in figure 5.

5. Analytical solutions for weak co-flows

Analytical solutions to the governing system of equations, (2.14), are now presented for highly forced ($\Gamma_0 \ll 1$) and highly lazy ($\Gamma_0 \gg 1$) releases into weak co-flows, specifically those that satisfy
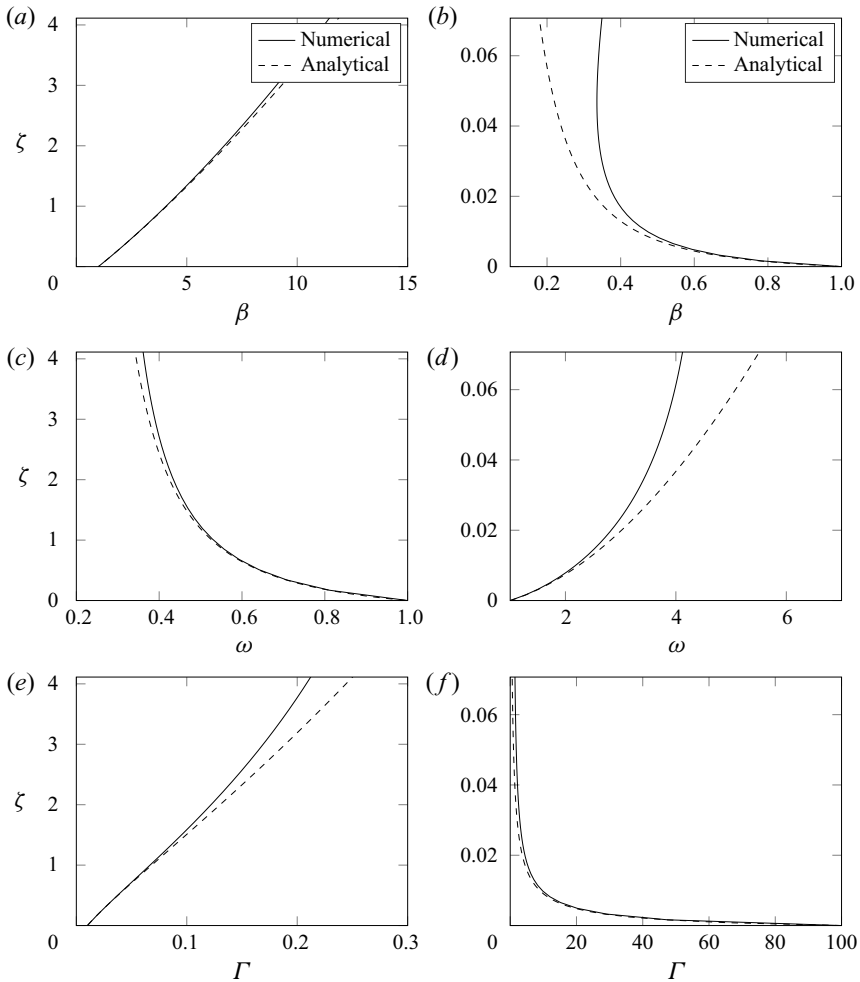
$$\Omega_0/\omega \ll 1. \tag{5.1}$$

932 A41-19

Figure 9. Values of β, ω and Γ. Solid lines represent the numerical solutions of (3.6). Dashed lines represent the analytical solutions for the limits of: (Left column) highly forced release in weak co-flow for ($\Gamma_0 = 0.01$, $\Omega_0 = 0.1$) (§ 5.1); (Right column) highly lazy release in weak co-flow for ($\Gamma_0 = 100$, $\Omega_0 = 0.1$) (§ 5.2).

To this end, the quadratic terms $(\Omega_0/\omega)^2$ are neglected in the governing equations (2.14).

These solutions, developed in § 5.1 and § 5.2 for $\beta(\zeta)$, $\omega(\zeta)$ and $\Gamma(\zeta)$, are plotted in figure 9 (dashed line) together with the numerical solutions of (2.14) (solid line). From (2.11) and (2.16), the dimensionless buoyancy is then known from $\beta(\zeta)$ and $\omega(\zeta)$:

$$\frac{g'}{g'_0} = \frac{\omega^2}{\beta}\frac{\Gamma}{\Gamma_0} = \frac{1}{\beta\omega}. \tag{5.2}$$

In order to account for the rapid dynamical variation of highly lazy releases toward their asymptotic states relative to the slow adjustment of highly forced releases, the individual analytical solutions are plotted over an identical dynamical range, rather than over an identical streamwise distance. Accordingly, the vertical axes in figure 9 span different ranges of ζ, ranges corresponding to those over which the Richardson number Γ varies from the source value to 50 % of the far-field value.

5.1. *Highly forced releases $\Gamma_0 \ll 1$*

For inertially dominated releases ($\Gamma \ll 1$), the governing equations (2.14) are simplified on making the approximation $1 - \Gamma \approx 1$ (cf. Hunt & Kaye 2005). The resulting coupled differential equations can then be straightforwardly solved to show

$$\Gamma = \frac{\Gamma_0}{\omega^3}, \tag{5.3a}$$

$$\beta = \frac{1}{\omega^{3/2}} \left(\frac{1 - 2\Omega_0}{\omega - 2\Omega_0} \right)^{1/2}, \tag{5.3b}$$

$$\zeta = \frac{(1 - 2\Omega_0)^{1/2}}{2\Omega_0^2} \left[\frac{(1 - \Omega_0/\omega)}{(1 - 2\Omega_0/\omega)^{1/2}} - \frac{1 - \Omega_0}{(1 - 2\Omega_0)^{1/2}} \right]. \tag{5.3c}$$

Re-arranging the latter for ω gives

$$\omega = \frac{\Omega_0}{1 - f + (f(f-1))^{1/2}} \quad \text{where } f = \left(\frac{2\Omega_0^2}{(1 - 2\Omega_0)^{1/2}} \zeta + \frac{1 - \Omega_0}{(1 - 2\Omega_0)^{1/2}} \right)^2. \tag{5.4}$$

As such, the streamwise variations $\beta(\zeta)$, $\omega(\zeta)$ and $\Gamma(\zeta)$ are known functions. Figure 9 (left column) plots the streamwise variations of (β, ω, Γ) from (5.3) for a representative forced release and weak co-flow. For the case shown, namely, ($\Gamma_0 = 0.01$, $\Omega_0 = 0.1$), the analytical solutions for β, ω and Γ remain within 10 % of the full numerical solution for $\zeta < 150$, $\zeta < 7.62$ and $\zeta < 2.65$, respectively. As we have taken $\alpha = 0.14$, $\zeta = 0.5$ is equivalent to a streamwise distance of 3.6 source widths.

5.2. *Highly lazy releases $\Gamma_0 \gg 1$*

For buoyancy dominated releases ($\Gamma \gg 1$, so that $\Gamma - 1 \approx \Gamma$) the governing equations (2.14) can again be simplified and solved to show that

$$\Gamma = \frac{\Gamma_0}{\omega^3}, \tag{5.5a}$$

$$\beta = \frac{1}{\omega} \left(\frac{\Gamma_0 + 2\Omega_0}{\Gamma_0 + 2\Omega_0\omega^2} \right)^{1/4}, \tag{5.5b}$$

$$\zeta = \frac{1}{2\Omega_0} \left[1 - \left(\frac{\Gamma_0 + 2\Omega_0}{\Gamma_0 + 2\Omega_0\omega^2} \right)^{1/4} \right]. \tag{5.5c}$$

The expression for ζ can be rearranged for ω, yielding

$$\omega = \left(\frac{\Gamma_0 + 2\Omega_0}{2\Omega_0(1 - 2\Omega_0\zeta)^4} - \frac{\Gamma_0}{2\Omega_0} \right)^{1/2}. \tag{5.6}$$

Figure 9 (right column) compares the analytical expressions in (5.5) and (5.6) with the numerical solutions to (2.14) for a representative highly lazy release issuing into a weak co-flow ($\Omega_0 = 0.1$, $\Gamma_0 = 100$). The analytical solutions for β, ω and Γ are within 10 % of the full numerical solutions for $\zeta < 0.016$, $\zeta < 0.027$ and $\zeta < 0.012$, respectively.

6. Conclusions

Given the inherent difficulties in providing an exact reproduction within the laboratory setting of a line source plume, or a sufficiently high aspect ratio source of finite width, with uniform release conditions along its entire length in a turbulence-free uniform co-flowing vertical stream, research has been hampered by a complete absence of detail surrounding their behaviour. Consequently, even a basic understanding of these flows had eluded us.

We set out to characterise how a co-flow affects the plume, specifically its growth rate, vertical velocity and dilution and, via the streamwise variation of the Richardson number, its dynamical variability. This important step was achieved by means of a theoretical model, whereby, the underlying governing conservation equations were derived based on a constant α-formulation and top-hat profiles for velocity and buoyancy. This simplified approach was taken so as to gain a first insight. The solutions of the governing equations were subsequently examined for the entire spectrum of possible source conditions, i.e. those spanning the classes of forced, pure and lazy plume releases.

Following this approach it proved possible to derive analytical solutions for highly forced and highly lazy releases in weak co-flows, as well as power-law solutions for the case of a line plume. These solutions agreed closely with the full solution obtained numerically. Based on our analysis, the behaviour of a plume in a co-flow was shown to be characterised by the source Richardson number, Γ_0, and the ratio of the co-flow and plume source velocities, Ω_0. Regarding the latter, we focused on entraining (rather than detraining) plumes which we reason require the co-flow to not exceed $\Omega_0 = 1$.

For all release conditions, the co-flow was shown to cause a reduction in the dilution relative to a plume with identical source conditions released into quiescent surroundings. This result has potentially wide implications, including to controlling the delivery of cool air from ceiling level (with minimal, or an absence of, dilution) to occupants in rooms by means of a shrouding stream of co-flowing air at ambient temperature.

In stark contrast to behaviour that is unique to lazy plumes in quiescent surroundings, we have shown that in the presence of a co-flow all three classes of release can contract to a neck in the near-source region before expanding downstream. We derived the minimum co-flow strength that produces necking behaviour and analysed the position and characteristics of the plume at the neck. Recognising that a co-flow causes a reduction in the relative velocity of the plume, contraction was expected given the acceleration of the plume fluid that stemmed from the associated strengthening of the buoyancy force relative to inertia.

Seeking the analogue of the dynamically invariant behaviour that is unique to pure plumes in quiescent surroundings, we have shown that dynamical invariance is possible only for forced releases ($\Gamma_0 < 1$) and deduced that unique to each is the co-flow strength $\Omega_0 = 1 - \sqrt{\Gamma_0}$ that leads to this invariance.

As a final note, the governing equations we consider are readily extended to the case of a non-constant entrainment coefficient. Indeed, a possible progression would be to reason for an entrainment model in which the entrainment coefficient varies with a suitably defined local Richardson number - the Richardson number and, thereby, the entrainment responding to the strength of the co-flow. Building in this way on the developments made herein would present a natural next step in further enhancing our understanding of these flows.

Author ORCIDs.
Ⓘ Gary R. Hunt https://orcid.org/0000-0001-9875-9274;
Ⓘ Jamie P. Webb https://orcid.org/0000-0002-1194-5582.

Appendix A. Conservation equations

Following the well-established route (Morton *et al.* 1956; Morton 1961), it is assumed that the turbulent plume flow can be described using mean flow variables. For the two-dimensional, slender and quasi-steady flow considered, the fundamental statements of mass and streamwise momentum conservation reduce to

$$\frac{\partial}{\partial x}(\rho u) + \frac{\partial}{\partial z}(\rho w) = 0 \quad \text{and} \quad \rho u \frac{\partial w}{\partial x} + \rho w \frac{\partial w}{\partial z} = -\frac{\partial P}{\partial z} + \rho g, \tag{A1a,b}$$

where $\partial P/\partial z$ is the streamwise pressure gradient. Combining the momentum and continuity equation allows the latter to be rewritten as

$$\frac{\partial}{\partial x}(\rho u w) + \frac{\partial}{\partial z}(\rho w^2) = -\frac{\partial P}{\partial z} + \rho g. \tag{A2}$$

Assuming that the hydrostatic pressure gradient of the environment is imposed on the plume, integrating from the centreline at $x = 0$ to the plume perimeter at $x = b/2$ yields

$$\frac{\mathrm{d}}{\mathrm{d}z} \int_0^{b/2} \rho w \, \mathrm{d}x + [\rho u]_{b/2} = 0 \quad \text{and} \quad \frac{\mathrm{d}}{\mathrm{d}z} \int_0^{b/2} \rho w^2 \, \mathrm{d}x + [\rho u w]_{b/2} = \int_0^{b/2} (\rho - \rho_a) g \, \mathrm{d}x. \tag{A3a,b}$$

Assuming top-hat profiles for velocity and buoyancy gives

$$\frac{\mathrm{d}}{\mathrm{d}z}[\rho b w] = 2\rho_a u_e \quad \text{and} \quad \frac{\mathrm{d}}{\mathrm{d}z}[\rho b w^2] = b g(\rho_a - \rho) + 2\rho_a w_a u_e. \tag{A4a,b}$$

On applying the Boussinesq approximation (A4) reduces to the statements of conservation of mass and momentum given in (2.3). Manipulating the internal energy equation (cf. Rooney & Linden 1996) leads to the following statement of conservation of volume for a two-dimensional non-Boussinesq plume:

$$\frac{\mathrm{d}}{\mathrm{d}z}[b w] = 2u_e. \tag{A5}$$

Combining (A5) with the statement of conservation of mass in (A4) and integrating yields

$$(\rho - \rho_a) b w = \text{const.} \tag{A6}$$

Multiplying by the constant g/ρ_a gives the left-hand side of (A6) the units of buoyancy flux per unit length and (A6) can then be rewritten as

$$\frac{\mathrm{d}}{\mathrm{d}z}\left[b w g \frac{(\rho_a - \rho)}{\rho_a} \right] = 0, \tag{A7}$$

which becomes the statement of conservation of buoyancy in (2.3) upon application of the Boussinesq approximation.
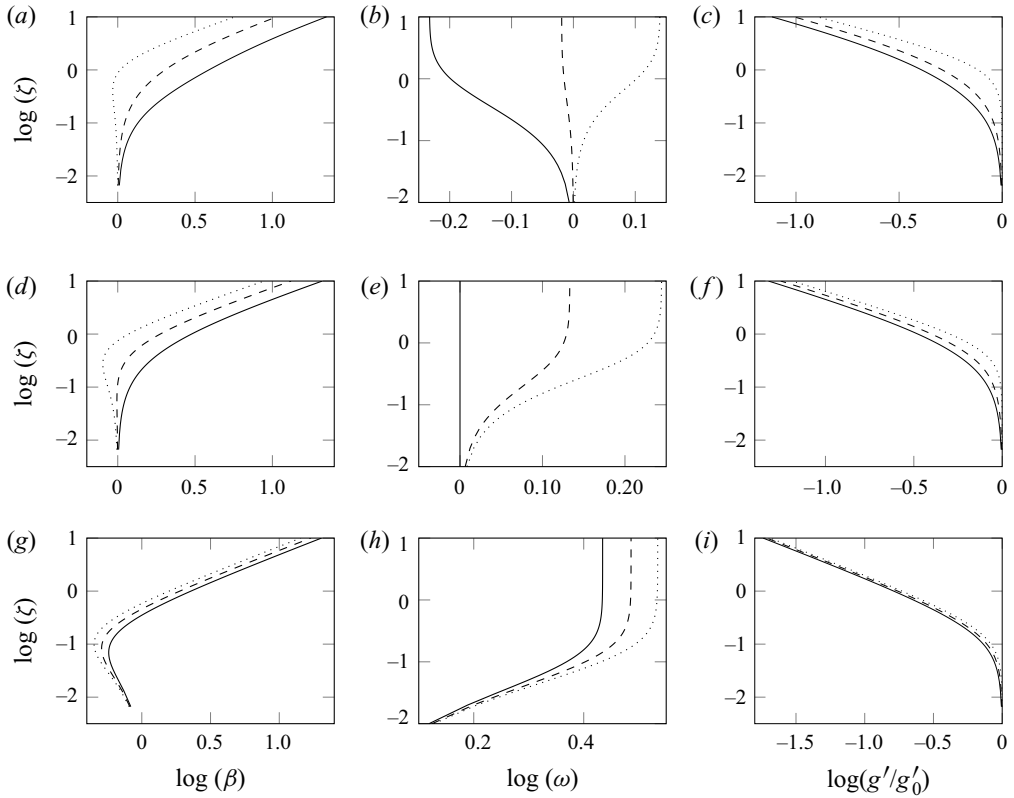
Figure 10. Log–log plots of β, ω and g'/g'_0 vs ζ. Solutions are shown for: $\Omega_0 = 0$ (———); $\Omega_0 = 0.5$ (- - - - - -); and $\Omega_0 = 1$ ($\cdots\cdots$); (a–c) $\Gamma_0 = 0.2$, (d–f) $\Gamma_0 = 1$ and (g–i) $\Gamma_0 = 20$.

Appendix B. Streamwise variation on log–log plots

The solutions shown in figures 5 and 6 are re-plotted in figure 10 on a log–log scale.

Appendix C. Pure releases in quiescent surroundings: $\Gamma_0 = 1$, $\Omega_0 = 0$

As expected, for the case where $\Omega = 0$ the governing equations (2.14) reduce to those derived by van den Bremer & Hunt (2014) for a motionless environment (the sole differences are factors of two which result from our scaling using the full width of the plume and van den Bremer & Hunt (2014) using the half-width). In this case, the solutions for pure releases are

$$\Gamma = 1, \quad \beta = \frac{b}{b_0} = 1 + 2\zeta, \quad \text{and} \quad \omega = \frac{w}{w_0} = 1. \qquad (C1a\text{–}c)$$

Noting that for this case $\Gamma_0 = \Gamma$, substituting for (2.11), and using the definition of g' in (1.1) yields

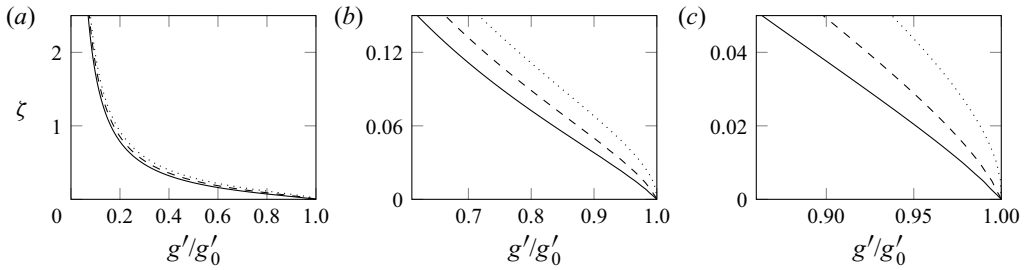$$\frac{\rho_a - \rho}{\rho_a - \rho_0} = \frac{1}{1 + 2\zeta}. \qquad (C2)$$

Figure 11. Successively magnified views of the dilution curves for a lazy release with $\Gamma_0 = 20$. Solutions are shown for: $\Omega_0 = 0$ (———); $\Omega_0 = 0.5$ (- - - - - -); and $\Omega_0 = 1$ (· · · · · · · ·). Note the reduction in the scale of the vertical axis between (*a*) and (*c*).
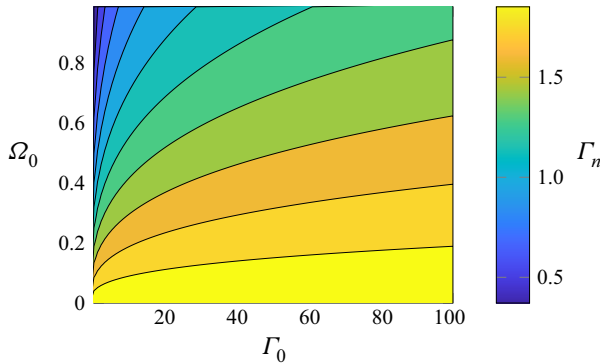

Figure 12. Variation of the Richardson number at the neck Γ_n with Γ_0 and Ω_0 from (E1). The plot shows contours of constant Γ_n with values as indicated by the colour bar.

Appendix D. Near-field dilution of lazy release

The near-source region of the dilution curves in figure 6 for the lazy release are shown in figure 11. The successively magnified views shown in (*a*)–(*c*) highlight that near-field dilution is weak for the co-flow $\Omega_0 = 1$ (dashed line).

Appendix E. Richardson number at the neck

A polynomial expression for the Richardson number at the neck $\Gamma = \Gamma_n$ is readily determined as follows. Substituting $d\beta/d\zeta = 0$ into (2.14*b*) yields $\Gamma_n = 2 - 3\Omega_0/\omega_n + \Omega_0^2/\omega_n^2$ and eliminating ω_n by means of (2.16), wherein $\omega_n = (\Gamma_0/\Gamma_n)^{1/3}$, gives

$$\Gamma_n - \frac{\Omega_0^2}{\Gamma_0^{2/3}}\Gamma_n^{2/3} + 3\frac{\Omega_0}{\Gamma_0^{1/3}}\Gamma_n^{1/3} - 2 = 0. \tag{E1}$$

The variation of Γ_n with Ω_0 and Γ_0 from (E1) is shown as a contour plot in figure 12. As co-flow strength increases, Γ_n decreases, rapidly for small Γ_0 and slowly by comparison as Γ_0 increases. For $\Omega_0 = 0$ this reduces to the established result that the neck occurs at $\Gamma_n = 2$ in the absence of a co-flow.

REFERENCES

AGRAWAL, A. & PRASAD, A.K. 2004 Evolution of a turbulent jet subjected to volumetric heating. *J. Fluid Mech.* **511**, 95–123.

ANWAR, H.O. 1969 Experiment on an effluent discharging from a slot into stationary or slow moving fluid of greater density. *J. Hydraul. Res.* **7**, 411–431.

BHAT, G.S. & NARASIMHA, R. 1996 A volumetrically heated jet: large-eddy structure and entrainment characteristics. *J. Fluid Mech.* **325**, 303–330.

BRADBURY, L.J.S. & RILEY, J. 1967 The spread of a turbulent plane jet issuing into a parallel moving airstream. *J. Fluid Mech.* **27**, 381–394.

VAN DEN BREMER, T.S. & HUNT, G.R. 2014 Two-dimensional planar plumes and fountains. *J. Fluid Mech.* **750**, 210–244.

CHEN, C.J. & RODI, W. 1980 *Vertical Turbulent Buoyant Jets: A Review of Experimental Data*, HMT, the Science and Applications of Heat and Mass Transfer, vol.4. Pergamon.

CSANADY, G.T. 1965 The buoyant motion within a hot gas plume in a horizontal wind. *J. Fluid Mech.* **22**, 225–239.

FAN, L.-N. 1967 Turbulent buoyant jets into stratified or flowing ambient fluids. PhD thesis, California Institute of Technology.

GASKIN, S. & WOOD, I.R. 2001 The axisymmetric and the plane jet in a coflow. *J. Hydraul. Res.* **39**, 451–458.

HILL, P.G. 1965 Turbulent jets in ducted streams. *J. Fluid Mech.* **22**, 161–186.

HOULT, D.P. & WEIL, J.C. 1972 Turbulent plume in a laminar cross flow. *Atmos. Environ.* **6**, 513–531.

HUNT, G.R. & VAN DEN BREMER, T.S. 2011 Classical plume theory: 1937–2010 and beyond. *IMA J. Appl. Math.* **76**, 424–448.

HUNT, G.R. & KAYE, N.B. 2005 Lazy plumes. *J. Fluid Mech.* **533**, 329–338.

KAYE, N.B. 2008 Turbulent plumes in stratified environments: a review of recent work. *Atmos.-Ocean* **46**, 433–441.

KOH, R.C.Y. & BROOKS, N.H. 1975 Fluid mechanics of waste-water disposal in the ocean. *Annu. Rev. Fluid Mech.* **7** (1), 187–211.

KOTSOVINOS, N.E. & LIST, E.J. 1977 Plane turbulent buoyant jets. Part 1. Integral properties. *J. Fluid Mech.* **81**, 25–44.

LEE, S.-L. & EMMONS, H.W. 1961 A study of natural convection above a line fire. *J. Fluid Mech.* **11**, 353–368.

MORTON, B.R. 1959 Forced plumes. *J. Fluid Mech.* **5**, 151–163.

MORTON, B.R. 1961 On a momentum-mass flux diagram for turbulent jets, plumes and wakes. *J. Fluid Mech.* **10**, 101–112.

MORTON, B.R., TAYLOR, G. & TURNER, J.S. 1956 Turbulent gravitational convection from maintained and instantaneous sources. *Proc. R. Soc. Lond. Ser.* A. *Math. Phys. Sci.* **234**, 1–23.

PAILLAT, S. & KAMINSKI, E. 2014 Entrainment in plane turbulent pure plumes. *J. Fluid Mech.* **755**, R2.

PAPPS, D.A. & WOOD, I.R. 1997 The effect of an intermittant flapping motion on the properties of merging plumes. *J. Hydraul. Res.* **35** (4), 455–472.

PARKER, D.A., BURRIDGE, H.C., PARTRIDGE, J.L. & LINDEN, P.F. 2020 A comparison of entrainment in turbulent line plumes adjacent to and distant from a vertical wall. *J. Fluid Mech.* **882** (A4), 1–35.

RAJARATNAM, N. & LAL, P.B.B. 1983 Plane turbulent plumes in coflowing streams. *J. Engng Mech.* **109**, 1299–1303.

RAMAPRIAN, B.R. & CHANDRASEKHARA, M.S. 1989 Measurements in vertical plane turbulent plumes. *J. Fluids Engng* **111**, 69–77.

RAMAPRIAN, B.R. & HANIU, H. 1989 Measurements in two-dimensional plumes in crossflow. *J. Fluids Engng* **111** (2), 130–138.

RILEY, D.S. & TVEITEREID, M. 1984 On the stability of an axisymmetric plume in a uniform stream. *J. Fluid Mech.* **142**, 171–186.

ROONEY, G.G. & LINDEN, P.F. 1996 Similarity considerations for non-Boussinesq plumes in an unstratified environment. *J. Fluid Mech.* **318**, 237–250.

ROUSE, H., YIH, C.S. & HUMPHREYS, H.W. 1952 Gravitational convection from a boundary source. *Tellus* **4** (3), 201–210.

SUBBARAO, E.R. & CANTWELL, B.J. 1992 Investigation of a co-flowing buoyant jet: experiments on the effect of Reynolds number and Richardson number. *J. Fluid Mech.* **245**, 69–90.

TAYLOR, G.I. 1945 Dynamics of a mass of hot gas rising in air. U.S. Atomic Energy Commission MDDC 919. LADC 276.

TURNER, J.S. 1966 Jets and plumes with negative or reversing buoyancy. *J. Fluid Mech.* **26**, 779–792.

TURNER, J.S. 1986 Turbulent entrainment: the development of the entrainment assumption, and its application to geophysical flows. *J. Fluid Mech.* **173**, 431–471.

WOOD, I.R., BELL, R.G. & WILKINSON, D.L. 1993 *Ocean Disposal of Wastewater*. World Scientific.

WOODS, A.W. 2010 Turbulent plumes in nature. *Annu. Rev. Fluid Mech.* **42**, 391–412.

WRIGHT, S. 1977 Mean behavior of buoyant jets in a crossflow. *J. Hydraul. Div. ASCE* **103**, 499–513.

YUAN, L.M. & COX, G. 1996 An experimental study of some line fires. *Fire Safety J.* **27** (2), 123–139.

ZELDOVICH, Y.B. 1937 The asymptotic laws of freely ascending convective flows. *Zh. Eksp. Teor. Fiz.* **7**, 1463–1465 (in Russian). English translation in *Selected Works of Yakov Borisovich Zeldovich*, **1**, 1992 (ed. J.P. Ostriker), 82–85, Princeton University Press.